JOURNAL OF GEOPHYSICAL RESEARCH, VOL. 103, NO. C8, PAGES 15,587–15,600, JULY 15, 1998

Primary production in Southern Ocean waters

Kevin R. Arrigo
Oceans and Ice Branch, NASA Goddard Space Flight Center, Greenbelt, Maryland

Denise Worthen
Science Systems and Applications, Inc., Lanham, Maryland

Anthony Schnell and Michael P. Lizotte
Department of Biology and Microbiology, University of Wisconsin Oshkosh, Oshkosh

Abstract. The Southern Ocean forms a link between major ocean basins, is the site of deep and intermediate water ventilation, and is one of the few areas where macronutrients are underutilized by phytoplankton. Paradoxically, prior estimates of annual primary production are insufficient to support the Antarctic food web. Here we present results from a primary production algorithm based upon monthly climatological phytoplankton pigment concentrations from the coastal zone color scanner (CZCS). Phytoplankton production was forced using monthly temperature profiles and a radiative transfer model that computed changes in photosynthetically usable radiation at each CZCS pixel location. Average daily productivity (g C m^{-2} d^{-1}) and total monthly production (Tg C $month^{-1}$) were calculated for each of five geographic sectors (defined by longitude) and three ecological provinces (defined by sea ice coverage and bathymetry as the pelagic province, the marginal ice zone, and the shelf). Annual primary production in the Southern Ocean (south of 50°S) was calculated to be 4414 Tg C yr^{-1}, 4–5 times higher than previous estimates made from in situ data. Primary production was greatest in the month of December (816 Tg C $month^{-1}$) and in the pelagic province (contributing 88.6% of the annual primary production). Because of their small size the marginal ice zone (MIZ) and the shelf contributed only 9.5% and 1.8%, respectively, despite exhibiting higher daily production rates. The Ross Sea was the most productive region, accounting for 28% of annual production. The fourfold increase in the estimate of primary production for the Southern Ocean likely makes the notion of an "Antarctic paradox" (primary production insufficient to support the populations of Southern Ocean grazers, including krill, copepods, microzooplankton, etc.) obsolete.

1. Introduction

Although phytoplankton play a major role in the carbon cycle, we know little of their seasonal and spatial distributions in the southern hemisphere or of the magnitude of their standing crop [*El-Sayed*, 1966; *Holm-Hansen et al.*, 1974; *Sakshaug and Holm-Hansen*, 1984; *Smith and Nelson*, 1986]. Much less is known about the rates of primary production in the Southern Ocean, and it is these rates which are essential to predicting the biogenic flux of CO_2 into the oceans. Estimates of annual primary production in the Southern Ocean have varied widely over the past 30 years as our understanding of Southern Ocean ecology has improved. Early estimates were based upon very few field measurements and ranged from 16 to 130 g C m^{-2} yr^{-1} [*Ryther*, 1963; *Bunt*, 1968, 1971]. Primary production for the entire Southern Ocean was estimated at 3000 Tg C yr^{-1} [*El-Sayed*, 1967]. However, these early estimates were considered biased because of a preponderance of samples collected within the high-productivity waters on the continental shelves. As more measurements were made in pelagic waters under nonbloom conditions, productivity estimates dropped about 80% to ~600 Tg C yr^{-1} [*Holm-Hansen et al.*, 1974; *El-Sayed*, 1978]. Later, the recognition that primary production is enhanced in the marginal ice zone (MIZ) led to arguments that another 141–383 Tg C yr^{-1} should be added to the annual estimate [*Smith and Nelson*, 1986; *Smith et al.*, 1988; *Legendre et al.*, 1992].

In the present study, a bio-optical algorithm has been used to estimate Southern Ocean primary productivity from algal pigments determined using the coastal zone color scanner (CZCS). This approach has several advantages over the use of standard in situ primary production methods alone. Whereas field campaigns are necessarily restricted both geographically and temporally, monthly climatological maps of pigment concentration determined using the CZCS provide a wealth of information about how phytoplankton are distributed over large areas and at relatively high spatial and temporal resolution. In addition, bio-optical productivity models can be modified over time to incorporate an increasingly sophisticated understanding of the physiology and ecology of polar organisms gained through field programs. Finally, productivity models facilitate the incorporation of environmental monitoring data such as space-based measurements of sea ice cover, sea surface temperature, phytoplankton pigments, wave height, and cloud cover, as well as meteorological data from a network of automated weather stations.

Paper number 98JC00930.
0148-0227/98/98JC-00930$09.00

2. Methods

2.1. Primary Productivity Algorithm

The algorithm calculates the rate of primary productivity (mg C m^{-3} h^{-1}) as a function of diurnal changes in spectral downwelling irradiance, water temperature (degrees Celsius), silicic acid or nitrate concentration (μmol L^{-1}), and chlorophyll *a* (Chl *a*) concentration (mg m^{-3}). Horizontal distributions of Chl *a* were determined from monthly CZCS climatologies for the period 1978–1986 [*Comiso et al.*, 1993, Plates 8 and 9]. It was assumed that Chl *a* concentration was uniform within the euphotic zone. Productivity at each CZCS pixel location was integrated over depth (at 0.5-m vertical resolution near the surface, increasing gradually to 5 m at the 1% light depth) and time (hourly for 24 hours) to determine daily primary productivity (mg C m^{-2} d^{-1}).

The radiative transfer model of *Gregg and Carder* [1990] was used to compute clear sky downwelling irradiance (E_{dclear}) at hour t, which was subsequently corrected (E_d) for fractional cloud cover (N) according to the equation [*Dobson and Smith*, 1988]

$$E_d(\lambda, t) = E_{\text{dclear}}(\lambda, t)[1 - 0.53(N^{0.5})]. \quad (1a)$$

Values for N were based on monthly climatologies obtained from *da Silva et al.* [1994].

Irradiance was propagated through the water column according to the equation

$$E_d(\lambda, z, t) = (1 - R)E_d(\lambda, t) \exp[-K_d(\lambda)z], \quad (1b)$$

where R is the surface reflection [*McClain et al.*, 1996], and

$$K_d(\lambda) = \frac{a_w(\lambda) + a_d(\lambda) + a_c^*(\lambda)\text{Chl } a + b_{bw}(\lambda) + b_{bp}(\lambda)}{\mu}, \quad (1c)$$

where μ is the mean cosine of the angular irradiance distribution, a is absorption, a_c^* is pigment specific absorption, b_b is backscatter, and the coefficients w, d, and p represent seawater, detritus, and particles, respectively.

Because the CZCS underestimated pigment concentrations in the Southern Ocean by approximately a factor of 2 [*Sullivan et al.*, 1993], a Southern Ocean CZCS correction factor was applied to the imagery as described by *Arrigo et al.* [1994]. Daily primary production (PP_{EU}, mg C m^{-2} d^{-1}) integrated to the depth of the base of the euphotic zone (D_E) was calculated as

$$PP_{EU} = \int_{z=0}^{D_E} \int_{t=0}^{24} \rho \text{ Chl } a(z) \frac{C}{\text{Chl } a}(z) G(z, t)\, dz\, dt, \quad (2)$$

where ρ is a measure of the active Chl *a* seen by the CZCS and is calculated as the ratio Chl *a*/(Chl *a* + phaeopigments) (assumed to be 1 unless otherwise noted), z is depth (meters), t is time (hours), C/Chl $a(z)$ is the elemental carbon to Chl *a* ratio (grams:grams) at a given depth (assumed to be 75 unless otherwise noted), and $G(z, t)$ is the net biomass-specific growth rate (hour^{-1}) at a given time and depth.

G was calculated as a function of the temperature-dependent upper limit to net growth, $G_{\max}$ (hour^{-1}), and the resource (either irradiance or nutrient) limitation term, r_{lim} (dimensionless), such that

$$G(z, t) = G_{\max}(z, t) r_{\text{lim}}(z, t). \quad (3)$$

$G_{\max}(z, t)$ was calculated according to the equation

$$G_{\max}(z, t) = G_0 \exp[rT(z)], \quad (4)$$

where G_0 is the microalgal net growth rate at 0°C (0.59 day^{-1}) and r is a rate constant (0.0633°C^{-1}) that determines the sensitivity of $G_{\max}$ to temperature, T (degrees Celsius) [*Eppley*, 1972]. $T(z)$ was obtained from the *Levitus et al.* [1994] 200-m means and held constant with depth. The resource limitation term, $r_{\text{lim}}(z)$, was calculated as the smaller of the nutrient limitation, N_{lim}, and light limitation, L, terms (the smaller will be most limiting,

$$r_{\text{lim}}(z, t) = \text{MINIMUM}[N_{\text{lim}}; L(z, t)]. \quad (5)$$

N_{lim} was determined using a dimensionless form of the *Monod* [1942] formulation,

$$N_{\text{lim}} = \frac{G}{G_{\max}} = \frac{N_s}{K_s + N_s} \quad (6)$$

where N_s is the annual climatological average concentration of silicic acid or nitrate in the upper 200 m determined from *Levitus et al.* [1994], K_s is the temperature-independent half-saturation constant for N_s (defined as the concentration of N_s where $G = 0.5G_{\max}$), and $G/G_{\max}$ describes the fraction of the maximum temperature-dependent growth rate allowed by N_s.

The light limitation term, $L(z, t)$, was calculated for each depth and each time step as

$$L(z, t) = 1 - \exp\left[-\frac{\text{PUR}(z, t)}{E_k'(z, t)}\right], \quad (7)$$

where PUR(z, t) is the photosynthetically usable radiation and $E_k'(z, t)$ is the spectral photoadaptation parameter [*Arrigo and Sullivan*, 1994]. Both PUR(z, t) and $E_k'(z, t)$ are in units of μmol photons m^{-2} s^{-1}. Phytoplankton growth is effectively light saturated when PUR $\approx 3E_k'$. PUR varies as a function of the spectral irradiance and the absorption characteristics of microalgae [*Morel*, 1978],

$$\text{PUR}(z, t) = \int_{\lambda=400}^{700} E_d(\lambda, z, t) \frac{a_c^*(\lambda)}{a_{\text{cmax}}^*} d\lambda, \quad (8)$$

where a_{cmax}^* is the maximum value attained by the phytoplankton absorption coefficient, $a_c^*(\lambda)$, and $E_d(\lambda, z, t)$ is the spectral downwelling irradiance at depth, z, and time, t. PUR(z, t) was used to calculate PUR*, a measure of the average amount of usable radiation available during the photoperiod, F, according to the equation

$$\text{PUR}^*(z) = \frac{\int_{t=12-F/2}^{12+F/2} \text{PUR}(z, t)\, dt}{F}. \quad (9)$$

$E_k'(z, t)$ in (7) varies as a function of PUR* according to the equations [*Arrigo and Sullivan*, 1994]

$$E_k'(z) = \frac{E_{k\max}'}{1 + 10 \exp[-B \text{ PUR}^*(z)]} \quad (10)$$

$$B = \exp[1.089 - 2.12 \log(E_{k\max}')], \quad (11)$$

where $E_{k\max}'$ is the maximum observed value for E_k'. *Lizotte and Arrigo* [1994] compiled spectral irradiance data and corresponding values of E_k' for phytoplankton collected over a wide

range of times, depths, and locations in the Southern Ocean and determined that $E'_{k\ max} \approx 80$ μmol photons m^{-2} s^{-1} (Figure 1). Equations (10) and (11) scale $E'_k(z)$ with depth to simulate photoadaptation such that $E'_k(z) \approx$ PUR* at intermediate depths (and irradiance levels) and asymptotically approaches $E'_{k\ max}$ and $E'_{k\ min}$ (= 26.4 μmol photons m^{-2} s^{-1} as defined in (10)) toward the surface and base of the euphotic zone, respectively.

2.2. Defining Regions of Interest

For the purpose of this study, the Southern Ocean (defined as the area south of 50°S) was divided into five geographic sectors and three open water ecological provinces. Geographic sectors were defined simply by longitude as described by *Gloersen et al.* [1992] and include the Weddell Sea (60°W–20°E), South Indian Ocean (20°–90°E), southwestern Pacific Ocean (90°–160°E), Ross Sea (160°E–130°W), and Bellingshausen-Amundsen Sea (130°–60°W) (Figure 2). The three ecological provinces were defined on the basis of sea ice coverage and bathymetry and include the pelagic, the MIZ, and the shelf (Plate 1).

Sea ice extent used to define ecological boundaries was determined from scanning multichannel microwave radiometer (SMMR) data using the algorithm described by *Gloersen et al.* [1992]. The boundary between open ocean and ice-covered waters was defined by the 10% sea ice concentration contour. Climatological sea ice extent for the period 1978–1986 was determined for the beginning and end of each month (the nearest available day to the beginning and end of each month was used). Sea ice boundaries were mapped to the CZCS grid, and each pixel within the monthly CZCS climatologies was then assigned to the appropriate geographic sector (e.g., Weddell Sea, Ross Sea, etc.) and ecological province (e.g., pelagic, MIZ, shelf).

The pelagic province was defined for a given month as the area between 50°S and the northernmost extent of the sea ice for that month; consequently, its size varies through time. Within the pelagic province is the permanently open ocean zone (POOZ), which extends from 50°S to the boundary of the annual maximum sea ice extent. Unlike the pelagic province, the area of the POOZ remains constant throughout the year.

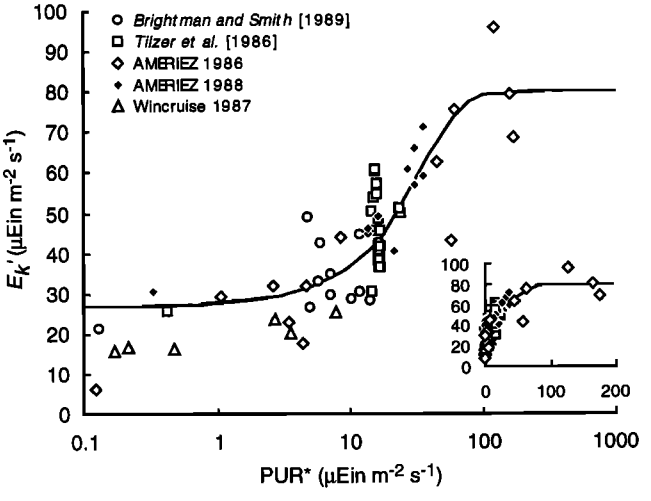

Figure 1. Variation in the spectral photoadaptation parameter (E'_k) for Antarctic phytoplankton as a function of mean daily photosynthetically usable radiation (PUR*).

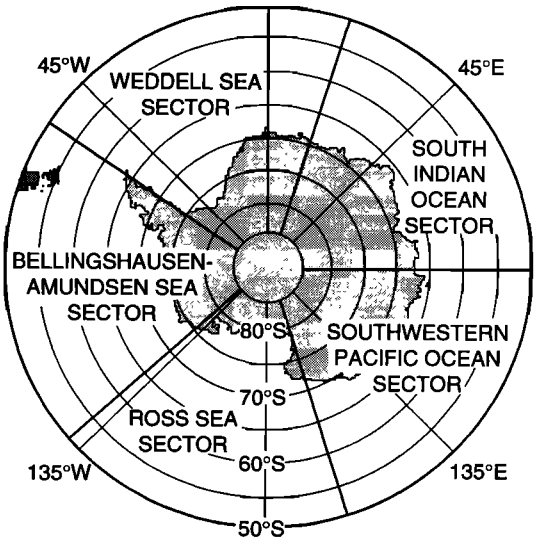

Figure 2. Map of the Southern Ocean showing the location of the five geographic sectors referred to in the text.

South of the pelagic province is the sea ice zone (SIZ), which contains the ecologically important MIZ. The MIZ is associated with the retreating sea ice edge and is defined operationally as the area where sea ice was present at the beginning of the month but not at the end. Because of the high temporal variability in the extent of the sea ice cover the size and location of the MIZ varies markedly by month. During those months when the sea ice area is expanding (March–October), the area of the MIZ is nearly zero. The shelf is defined as open waters <1000 m deep; however, wherever the MIZ extends onto the shelf, any productivity there is treated as MIZ production rather than shelf production (to avoid double counting). The portions of the Patagonian and New Zealand shelves which extend south of 50°S were excluded from all analyses to avoid confusion with productivity on the Antarctic continental shelf.

Occasionally, a CZCS pixel (presumed to be open water) is coregistered with a sea ice pixel from the SMMR. This was possible because the monthly CZCS climatologies include all valid pixels within a given month during the CZCS mission (1978–1986). Because the ice-free area for a given month varied from year to year, the monthly CZCS climatology represents the maximum open water area during that month between the years 1978 and 1986. In contrast, the sea ice extent was determined as the average ice extent at the beginning and end of each month during the same time period (1978–1986). Because the extent of open water is larger in the CZCS imagery than in the annually averaged SMMR data, some CZCS pixels were registered with ice cover. To correct this problem, any CZCS pixel located in an area of new sea ice growth (where sea ice was present at the end but not the beginning of the month) was either assigned to the shelf or to the pelagic province, depending upon water depth. All other sea-ice-associated CZCS pixels were assigned to the MIZ.

2.3. CZCS Data Coverage

Because of infrequent sampling and extensive cloud cover, segments of the Southern Ocean each month were never sampled during the CZCS mission. Fractional coverage by month for each geographic sector and ecological province in the Southern Ocean are shown in Table 1. Because the present

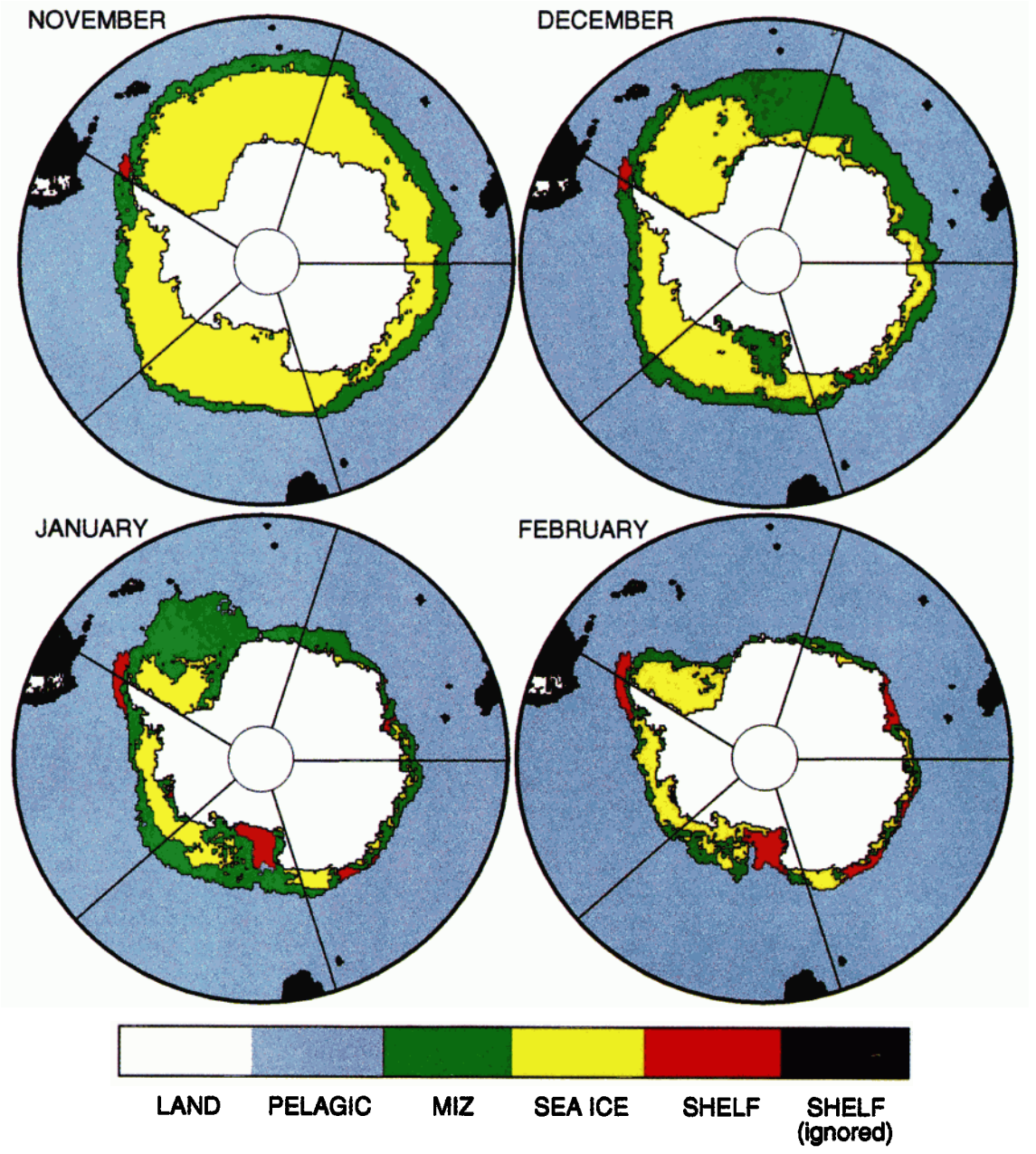

Plate 1. Map of the Southern Ocean showing the position of the three ecological provinces (pelagic, marginal ice zone, and shelf) during the most productive months of spring and summer.

study is concerned, in part, with the spatial variation in Southern Ocean primary production, the incomplete CZCS coverage required that the rate of carbon fixation be averaged at no shorter than monthly timescales. Therefore monthly primary production in each geographic sector and ecological province was calculated as the product of its spatially averaged rate of production and its areal extent for that month.

2.4. Model Parameterization and Validation

Prior to its utilization with CZCS data, algorithm output was compared to in situ estimates of daily production at stations within the Southern Ocean for which all necessary ancillary data (latitude, longitude, date, temperature, biomass, daily dose of PAR) were available. The in situ data were obtained from the primary productivity data archive at the Brookhaven National Laboratory as maintained by M. Behrenfeld and P. Falkowski [*Behrenfeld and Falkowski*, 1997a]. The slope (1.002) of the regression of in situ versus algorithm-derived primary production was not significantly different from unity ($p < 0.00001$, $n = 26$) and explained >70% of the variance (Figure 3a). The root-mean-square error was 0.087 g C m^{-2} d^{-1}. Although simpler primary productivity algorithms are able to achieve a similar level of agreement with in situ measurements, the algorithm described here allows a more detailed investigation of the effect of various environmental variables on estimated rates of production.

3. Results

3.1. Temporal Changes in the Size of the Ecological Regimes

The pelagic province, ranging in size from 23.8 × 10^6 to 38.7 × 10^6 km^2, is always much larger than either the MIZ or

Table 1. Total Area and the Ratio of CZCS Pixel Area to Total Area in the Southern Ocean

Month	Weddell Sea	South Indian Ocean	Southwestern Pacific Ocean	Ross Sea	Bellinghausen-Amundsen Sea	Total Southern Ocean
			Pelagic			
July	3.88 (0.07)	4.62 (0.01)	5.86 (0.08)	5.83 (0.20)	5.83 (0.08)	25.76 (0.09)
August	3.42 (0.08)	4.15 (<0.01)	5.27 (0.19)	5.56 (0.23)	5.59 (0.08)	24.00 (0.13)
September	3.51 (0.32)	3.85 (0.32)	5.18 (0.27)	5.56 (0.52)	5.68 (0.32)	23.78 (0.35)
October	3.52 (0.41)	3.89 (0.50)	5.23 (0.18)	5.86 (0.39)	5.67 (0.27)	24.17 (0.34)
November	4.09 (0.90)	4.10 (0.58)	5.49 (0.61)	6.03 (0.56)	5.88 (0.47)	25.58 (0.61)
December	4.79 (0.85)	5.26 (0.44)	6.36 (0.54)	6.48 (0.51)	6.31 (0.33)	29.20 (0.52)
January	7.03 (0.63)	6.93 (0.66)	6.80 (0.93)	7.48 (0.70)	6.83 (0.81)	35.06 (0.75)
February	8.91 (0.88)	7.21 (0.86)	6.91 (0.86)	8.44 (0.48)	7.19 (0.51)	38.66 (0.72)
March	8.45 (0.83)	7.18 (0.70)	6.89 (0.85)	7.87 (0.49)	7.02 (0.65)	37.41 (0.70)
April	7.40 (0.51)	6.78 (0.30)	6.58 (0.63)	7.07 (0.20)	6.64 (0.32)	34.47 (0.39)
May	6.00 (0.12)	6.05 (0.11)	6.25 (0.09)	6.60 (0.16)	6.48 (0.37)	31.37 (0.10)
June	4.89 (0.05)	5.20 (ND)	5.90 (0.02)	6.10 (0.07)	6.10 (ND)	28.19 (0.03)
			MIZ			
September	0.22 (1.32)	0.02 (>5)	0.02 (ND)	0.23 (ND)	0.06 (0.44)	0.56 (0.75)
October	0.70 (0.63)	0.18 (1.01)	0.20 (0.09)	0.18 (0.28)	0.14 (0.79)	1.40 (0.57)
November	0.73 (1.53)	1.13 (0.28)	0.84 (0.33)	0.41 (0.03)	0.36 (0.73)	3.47 (0.57)
December	2.12 (0.70)	1.68 (0.53)	0.46 (0.71)	1.24 (0.55)	0.48 (0.70)	5.98 (0.62)
January	1.89 (0.91)	0.39 (1.56)	0.23 (1.93)	0.98 (1.04)	0.41 (1.21)	3.90 (1.09)
February	0.25 (1.85)	0.14 (2.09)	0.11 (1.52)	0.22 (1.84)	0.11 (2.22)	0.84 (1.89)
March	<0.01 (>5)	0.04 (3.34)	<0.01 (>5)	<0.01 (>5)	0.01 (>5)	0.05 (>5)
			Shelf			
November	0.07 (1.00)	0.00 (ND)	0.00 (ND)	0.00 (ND)	0.00 (ND)	0.07 (1.00)
December	0.09 (1.01)	<0.01 (ND)	0.02 (0.86)	0.01 (0.80)	0.01 (1.00)	0.13 (0.96)
January	0.11 (0.98)	0.05 (1.05)	0.08 (1.01)	0.37 (0.87)	0.08 (0.96)	0.69 (0.93)
February	0.11 (1.02)	0.13 (1.08)	0.19 (0.92)	0.34 (0.93)	0.12 (0.91)	0.87 (0.96)
March	0.09 (1.17)	0.05 (2.16)	0.13 (1.18)	0.02 (3.77)	0.15 (1.05)	0.44 (1.35)
April	0.06 (0.27)	0.01 (ND)	0.01 (ND)	<0.01 (ND)	0.13 (0.01)	0.21 (0.09)

The ratio is given in parentheses. Areas are in units of 10^6 km^2. ND, no data from the coastal zone color scanner (CZCS). Ratios >1 arise when numerous CZCS pixels are reassigned from ice-covered waters to the other ecological provinces. Very high ratios (>2.0) were rare, resulting when the area of open water was minimal (e.g., September in the marginal ice zone (MIZ)).

the shelf (Table 1) because of the large area of the POOZ (23.8×10^6 km^2). The MIZ, a component of the SIZ (20×10^6 km^2), is short-lived and variable in size and present (by definition) only when and where the sea ice has retreated. It attains its maximum extent of 6×10^6 km^2 in December. The continental shelf is a small area restricted to coastal Antarctica and the Scotia Shelf. For most of the year this region is covered by ice, but it becomes ice free between November and April, attaining a maximum size of 0.9×10^6 km^2. The maximum area of the pelagic province (in February) is >6 times larger than the maximum MIZ area (in December) and >44 times the peak shelf area (in February).

The amount of seasonal variation in the size of the pelagic zone differs for each geographic sector (Table 1). The Ross Sea has the greatest pelagic area during the peak primary production months of summer, while the Weddell Sea exhibited the largest annual shift in the size of the pelagic province, because of its large seasonal change in sea ice extent. The maximum sea ice extent in the Weddell Sea (6.1×10^6 km^2) is up to 6 times larger than the maximum ice extent of the other four sectors [*Arrigo et al.*, 1998]. The recession of the ice pack by the end of summer increases the pelagic area of the Weddell Sea by $\sim 5.5 \times 10^6$ km^2. The ocean surface area of the next largest region, the South Indian Ocean, increases by $\sim 3.4 \times 10^6$ km^2 between winter and summer. In contrast, the pelagic region of the Bellingshausen-Amundsen Sea sector undergoes very little change during the course of a year ($\sim 1.6 \times 10^6$ km^2). The area of the southwestern Pacific Ocean sector also changes little over the year and contains the smallest pelagic area during the four most biologically productive months of the summer-fall.

The size of the MIZ in each sector is related to changes in ice cover. Thus the large retreat of the sea ice cover in the Weddell Sea sector during the spring-summer produces the largest MIZ (2.12×10^6 km^2) area of any sector for a given month (Table 1). The South Indian Ocean MIZ area is the second largest at nearly 1.68×10^6 km^2, while the Bellingshausen-Amundsen Sea sector has the smallest MIZ area (peak of 0.48×10^6 km^2 in December).

The distribution of shelf regions in each sector depends on both bathymetry and the annual variation in sea ice extent. The Ross Sea has the largest area of open water over the shelf (Table 1) containing 54% of the Southern Ocean shelf area in January. The largest single-month increase in shelf is also seen in the Ross Sea sector (November–December, Figure 2, Plate 1, and Table 1) owing to rapid formation of the spring polynya. For both the Ross Sea and the Bellingshausen-Amundsen Sea (including the western margin of the Antarctic Peninsula), large portions of the shelves are covered by multiyear ice [*Arrigo et al.*, 1998]. For most of the year the South Indian Ocean has the smallest shelf area.

3.2. Primary Production

Overall, average, modeled rates of primary production in the Southern Ocean (Table 2) ranged from 0.075 g C m^{-2} d^{-1} in the pelagic province of the Weddell Sea in June to 3.94 g C m^{-2} d^{-1} on the shelf of the Ross Sea in December. All geographic sectors and ecological provinces exhibited peak pro-

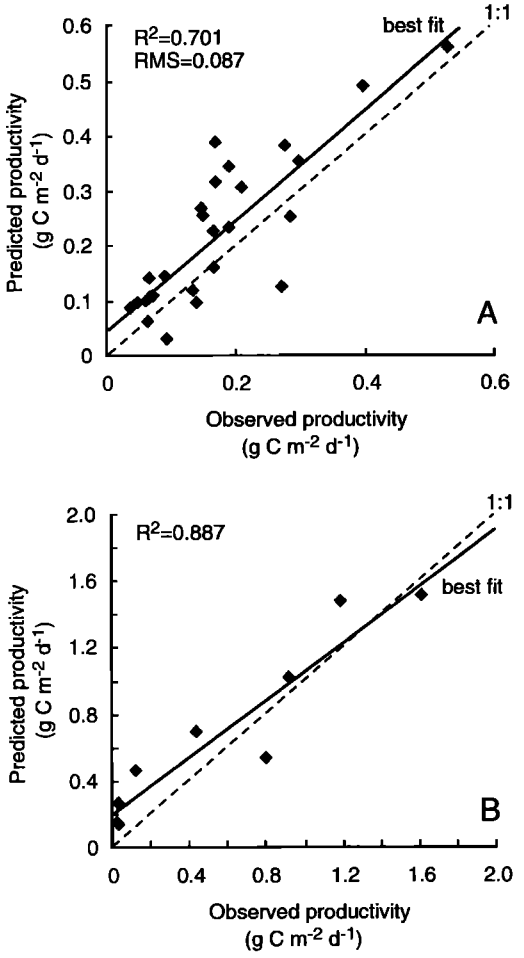

Figure 3. Comparison of algorithm output with (a) in situ estimates of daily production at 26 oceanographic stations within the Southern Ocean and with (b) in situ estimates of daily production averaged by ecological province and by month (see Table 5).

duction rates in December or January (summer). The highest daily production rates were associated with the shelf in all sectors except the Bellingshausen-Amundsen Sea, which had slightly higher primary production in the MIZ. The maximum monthly average rate of production on the shelf (3.94 g C m^{-2} d^{-1}) was over 4 times the pelagic maximum monthly average rate (0.83 g C m^{-2} d^{-1}).

Of the three ecological provinces addressed here, daily primary production in the pelagic province was the lowest, averaging <0.4 g C m^{-2} d^{-1}. However, during the austral autumn and winter when sea ice is actively growing (no MIZ) and the continental shelf regions are sea-ice-covered, the bulk of the primary production in the Southern Ocean is associated with the pelagic province. The pelagic province in the Ross Sea sector was the most productive, with maximum daily rates of production of 0.82 g C m^{-2} d^{-1} in December. The Weddell Sea was nearly as productive, exceeding 0.7 g C m^{-2} d^{-1} in December. Primary production within the pelagic province of the South Indian Ocean was lowest, remaining <0.5 g C m^{-2} d^{-1} throughout the year.

In three of the five geographic sectors (Weddell Sea, Ross Sea, and South Indian Ocean), daily rates of production within the MIZ were intermediate between rates measured on the shelf and in the pelagic province (Table 2). In the other two geographic sectors (SW Pacific Ocean and the Bellingshausen-Amundsen Sea), daily productivity within the MIZ was approximately equal to productivity on the shelf. The Ross Sea MIZ was the most productive, with a peak rate of 1.69 g C m^{-2} d^{-1}, while the Weddell Sea exhibited maximum rates only half as high (0.82 g C m^{-2} d^{-1}). In contrast to the shelf and pelagic provinces, the rate of daily primary production in the MIZ generally peaked a month or more after maximum melt back of the annual sea ice. It was at this time that the MIZ had retreated all the way back to the Antarctic coast, suggesting that primary production in the MIZ is greatest when the MIZ is located over shallow waters.

Annual water column primary production in the Southern Ocean (all area south of 50°S) was calculated to be 4414 Tg C yr^{-1} (Table 3). The Ross Sea sector had the highest annual production (1222 Tg C yr^{-1}) of any geographic sector, accounting for nearly 28% of the annual production of the Southern Ocean. Although the pelagic province and the MIZ of the Weddell Sea were larger in area (the MIZ was nearly twice as large), this was more than compensated for by higher rates of production per unit area in the Ross Sea. The Ross Sea also had the largest and most productive shelf of any sector. The other geographic sectors contributed between 14 (South Indian Ocean) and 23% (Weddell Sea) to annual primary production in the Southern Ocean. MIZ production was greatest in the Weddell Sea, where it accounted for 13.1% of the annual primary production in that sector, and was least important in the Bellingshausen-Amundsen Sea, amounting to only 5.6% of annual production. The proportion of production on the shelf was greatest in the Ross Sea (2.5% of annual Ross Sea primary production) and smallest in the SW Pacific Ocean (1.2% of annual primary production).

Primary production was greatest in December (816 Tg C $month^{-1}$) as rates of production peaked in the MIZ and the pelagic province (Table 4). All sectors and ecological provinces exhibited a seasonal pattern of primary production which was driven primarily by solar irradiance and secondarily by sea ice coverage. The pelagic region contributed 88.6% of the total annual primary production (Table 4) while the MIZ and the shelf contributed 9.5% and 1.8%, respectively, despite the higher daily production rates in the latter two provinces (Table 2). The low contribution of the shelf and MIZ to total annual production was due to the limited spatial and temporal coverage of these provinces (Table 1). The MIZ was present only when the sea ice was retreating (September through March), and the shelf was productive only when it was ice free (November through April). On a monthly basis the MIZ was most important in December when it accounted for 23% of the total December primary production, while the importance of the shelf peaked in January, when it accounted for 4.0% of production.

Overall, primary production in permanently open waters (POOZ) was larger than that contributed by seasonally ice-covered regions (SIZ), the former making up 67% of the Southern Ocean total. By sector the Weddell Sea was the only region in which SIZ productivity (54%) was greater than POOZ productivity (46%); for the other four sectors the POOZ contribution ranged from 61 to 77% of the total. POOZ always contributed the majority of the annual production in the pelagic province (overall, 72% of the pelagic province total, ranging from 57% in the Weddell Sea to 84% in the Bellingshausen-Amundsen Sea).

Table 2. Daily Primary Productivity for the Southern Ocean

Month	Weddell Sea	South Indian Ocean	Southwestern Pacific Ocean	Ross Sea	Bellinghausen-Amundsen Sea	Total Southern Ocean
			Pelagic			
July	0.15	0.08	0.12	0.18	0.10	0.15
August	0.18	0.18	0.24	0.28	0.31	0.26
September	0.28	0.50	0.24	0.27	0.25	0.30
October	0.46	0.25	0.35	0.43	0.35	0.37
November	0.61	0.45	0.44	0.75	0.46	0.55
December	0.70	0.50	0.53	0.82	0.98	0.69
January	0.67	0.42	0.37	0.64	0.61	0.53
February	0.67	0.40	0.33	0.47	0.41	0.47
March	0.43	0.29	0.30	0.50	0.31	0.36
April	0.29	0.14	0.24	0.57	0.14	0.26
May	0.25	0.10	0.21	0.20	0.09	0.19
June	0.08	ND	0.22	0.15	ND	0.14
			MIZ			
September	0.32	0.48	ND	ND	0.14	0.35
October	0.70	0.23	0.24	0.28	0.32	0.50
November	0.54	0.46	0.85	1.47	0.77	0.61
December	0.76	0.89	1.13	1.69	1.08	1.02
January	0.83	0.96	1.18	0.92	1.39	0.97
February	0.75	0.61	0.85	0.66	0.81	0.72
March	0.46	0.46	0.62	0.33	0.74	0.47
			Shelf			
November	0.72	ND	ND	ND	ND	0.72
December	1.44	ND	0.96	3.94	1.21	1.52
January	1.17	2.04	1.19	1.63	1.19	1.48
February	1.29	1.43	0.59	0.99	1.00	1.02
March	0.84	1.00	0.36	0.45	0.95	0.72
April	0.60	ND	ND	ND	0.82	0.61

Primary productivity in units of g C m^{-2} d^{-1}. ND, no data from CZCS.

4. Discussion

4.1. Comparison With Other Estimates: In Situ

Although in situ measurements of primary production in the Southern Ocean are sparse, there are a number of studies with which the algorithm-derived estimates presented here can be compared (Table 5). Unfortunately, none of these studies measured the ancillary information required to make a station-by-station comparison with algorithm estimates. However, if production estimates from many investigations are combined and averaged by month and by ecological province, then a comparison with algorithm output is possible. Results of this analysis demonstrate good agreement between in situ and algorithm-based estimates of primary productivity (Figure 3b and Table 5). Both techniques indicate that daily rates of production are highest on the continental shelf in December and January, averaging about 1.5 g C m^{-2} d^{-1}, and lowest in the open ocean in the austral winter. The slope of 0.85 and positive intercept of 0.20 g C m^{-2} d^{-1}, which result when algorithm output is regressed against in situ observations, suggest that the model may overestimate productivity during the winter in the pelagic province. This is not a serious problem, however, because the combined production in June, July, and August accounts for only 10% of the annual production in the pelagic province in the Southern Ocean (Table 4).

Our estimates of primary production in the MIZ agree well with measurements made in situ in both the Weddell and the Ross Sea. *Smith and Nelson* [1986] reported primary productivity within an ice edge bloom in the Weddell Sea averaging 0.571 g C m^{-2} d^{-1} based upon ^{14}C uptake rates. *Jennings et al.* [1984], using the observed nutrient depletion during that same

Table 3. Annual Primary Production in the Southern Ocean

Regime	Weddell Sea	South Indian Ocean	Southwestern Pacific Ocean	Ross Sea	Bellingshausen-Amundsen Sea	Total Southern Ocean
Pelagic	858	543	665	1076	770	3912
POOZ	465	384	556	880	635	2942
MIZ	132	77	51	116	46	422
Shelf	17	10	8	30	15	80
Total	1007	630	724	1222	831	4414

Primary production in units of Tg C yr^{-1}. Estimates are presented for the three ecological provinces defined in this paper and for the permanently open ocean zone (POOZ), a subsection of the pelagic province. Seasonal ice zone (SIZ) productivity can be estimated from the difference between Total and POOZ for each column.

Table 4. Monthly Primary Production in the Southern Ocean

Month	Weddell Sea	South Indian Ocean	Southwestern Pacific Ocean	Ross Sea	Bellinghausen-Amundsen Sea	Total Southern Ocean
			Pelagic			
July	18.2	11.0	20.7	31.9	17.7	99.5
August	17.4	20.9	35.1	43.3	48.7	165.4
September	30.1	59.1	39.2	47.3	44.1	219.8
October	48.6	29.1	54.3	75.8	59.6	267.4
November	77.4	56.7	74.9	139.2	84.0	432.2
December	101.1	77.2	101.4	158.4	184.6	622.7
January	146.8	89.6	77.8	147.4	129.6	591.2
February	186.1	89.0	71.3	122.1	90.9	559.4
March	108.9	61.8	61.4	117.0	64.6	413.7
April	67.2	29.7	48.8	125.4	28.3	299.4
May	44.6	18.8	39.9	39.8	17.6	160.7
June	11.4	ND	40.3	28.7	ND	80.4
Total						3911.8*
			MIZ			
September	2.2	0.3	ND	ND	0.3	2.7
October	14.5	1.3	1.42	1.6	1.4	20.1
November	12.4	16.1	22.1	18.9	8.5	77.9
December	48.5	44.7	15.6	62.6	15.7	187.2
January	48.3	11.6	8.4	27.9	17.7	113.9
February	5.9	2.6	3.0	4.6	2.8	18.8
March	<0.1	0.5	<0.1	<0.1	0.2	0.8
Total						421.4†
			Shelf			
November	1.5	ND	ND	ND	ND	1.5
December	3.9	ND	0.6	1.18	0.4	6.1
January	4.0	3.5	3.0	18.6	3.0	31.9
February	4.1	5.6	3.4	10.3	3.7	27.2
March	2.3	1.4	1.4	0.3	4.1	9.6
April	1.2	ND	ND	ND	3.3	4.5
Total						80.7‡

Primary production in units of Tg C month^{-1}. ND, no data from CZCS.
*Total is 88.6% of annual production.
†Total is 9.5% of annual production.
‡Total is 1.8% of annual production.

bloom, calculated a production rate of 0.566 g C m^{-2} d^{-1}. Both of these estimates are within 4% of our average spring-summer value of 0.588 g C m^{-2} d^{-1} for the MIZ of the Weddell Sea. In 1983, *Wilson et al.* [1986] investigated an ice edge phytoplankton bloom in the Ross Sea and reported that average primary productivity was 0.962 g C m^{-2} d^{-1}, within 8% of our estimate of 0.891 g C m^{-2} d^{-1}.

Previous calculations of annual production within the entire Southern Ocean MIZ range from 141 [*Legendre et al.*, 1992] to 383 Tg C yr^{-1} [*Smith and Nelson*, 1986]. Surprisingly, the primary difference between these two estimates is not the productivity per unit area assumed by each (which is actually much higher in work by *Legendre et al.* [1992]) but the size of the MIZ used in each calculation. *Legendre et al.* [1992] calcu-

Table 5. Comparison of Monthly Averaged Primary Production in the Southern Ocean Measured In Situ and Estimated by the Productivity Algorithm

Ecological Province	Month	In Situ Mean (±s.d.)	*n*	Algorithm Mean (±s.d.)	Reference
Pelagic	January	0.81 (0.50)	13	0.53	*El-Sayed* [1967]
Pelagic	June	0.04 (0.02)	13	0.13	*El-Sayed* [1967], *Cota et al.* [1992]
Pelagic	July	0.03 (0.02)	14	0.14	*Cota et al.* [1992]
Pelagic	August	0.04 (0.02)	8	0.26	*Cota et al.* [1992]
Pelagic	December	0.44 (0.56)	11	0.69	*El-Sayed* [1967]
Shelf	January	1.19 (1.22)	28	1.48	*El-Sayed* [1967], *El-Sayed and Mandelli* [1965], *Mitchell and Holm-Hansen* [1991], ROAVERRS 96–97 (M. P. Lizotte and K. R. Arrigo, unpublished data, 1997)
Shelf	February	0.93 (1.48)	9	1.02	*El-Sayed* [1967], *El-Sayed and Mandelli* [1965], *Mitchell and Holm-Hansen* [1991]
Shelf	December	1.62 (1.09)	21	1.51	*El-Sayed* [1967], *El-Sayed and Mandelli* [1965], *Mitchell and Holm-Hansen* [1991], ROAVERRS 96–97 (M. P. Lizotte and K. R. Arrigo, unpublished data, 1996)
MIZ	March	0.12 (0.08)	14	0.46	AMERIEZ 86 (W. O. Smith, unpublished data, 1986)

ROAVERRS is research on ocean-atmosphere variability and ecosystem response in the Ross Sea.

lated the MIZ area for each season as a product of the ice edge length (the circumference of the ice edge) and MIZ width (100 km). *Smith and Nelson* [1986] used the area uncovered each month during the annual sea ice retreat using SMMR data to estimate the size of the MIZ, a procedure that yields a much larger MIZ area than that calculated by *Legendre et al.* [1992] during the highly productive spring and summer months. For example, the area of the MIZ estimated by *Smith and Nelson* [1986] for the months of November, December, January, and February was 2.28×10^6 km^2, 6.84×10^6 km^2, 4.34×10^6 km^2, and 2.37×10^6 km^2, respectively, compared to the value of 1.75×10^6 km^2 used by *Legendre et al.* [1992] for the same time period. Substituting a more realistic MIZ width of 250 km [*Smith and Nelson*, 1986] into the calculation of MIZ area by *Legendre et al.* [1992] yields a revised annual production estimate for the MIZ of 345 Tg C yr^{-1}, much closer to the estimate of *Smith and Nelson* [1986].

The estimate of annual MIZ primary production (413 Tg C yr^{-1}) computed in the present study by the productivity algorithm is within 8% of the value (383 Tg C yr^{-1}) calculated by *Smith and Nelson* [1986] and exhibited an identical monthly trend (Figure 4). This is not surprising considering that our approach for estimating the area of the MIZ was fundamentally the same as that of *Smith and Nelson* [1986] and that our daily production rates calculated for the Weddell Sea and the Ross Sea were similar to theirs. However, the average production rate (0.767 g C m^{-2} d^{-1}) calculated for the entire Antarctic MIZ by *Smith and Nelson* [1986] was based on productivity data collected in the Weddell and Ross Seas only. Given that the mean productivity in these two sectors differs by nearly a factor of 2 (0.571 g C m^{-2} d^{-1} for the Weddell Sea and 0.962 g C m^{-2} d^{-1} for the Ross Sea), there was no a priori reason to believe that their combined mean would be representative of the entire Southern Ocean MIZ. However, our study suggests that these two geographic sectors do indeed appear to represent the extremes in rates of daily production within the Southern Ocean (Table 2) and that the combined average for these two sectors computed by *Smith and Nelson* [1986] is similar to our calculated mean for the entire Southern Ocean MIZ (0.834 g C m^{-2} d^{-1}).

4.2. Comparison With Other Estimates: Satellite

Our annual primary production estimate of 4414 Tg C yr^{-1} for the Southern Ocean is consistent with earlier satellite-based estimates which vary from 4000 to 9150 Tg C yr^{-1} [*Behrenfeld and Falkowski*, 1997a, Table 2] (Table 6 in the present paper). The greater than twofold variability in these estimates reflects the different approaches used in these studies to estimate primary production from ocean color satellite data. Differences exist not only in the specific algorithm formulations used in each study (which will be discussed later), but also in the specification of the Southern Ocean boundaries, the treatment of CZCS data used to represent the pigment fields, the use of sea ice masks, and the sources of ancillary input data such as temperature, irradiance, cloud cover, wind speeds, nutrients, etc. The twofold range in estimates of Southern Ocean primary production can be reduced substantially simply by specifying consistent boundaries and input fields for all primary productivity algorithms.

The approach used in the present study was to define the boundaries of relevant ecological provinces and geographic sectors by using monthly climatological SMMR-derived sea ice concentration data. Productivity values for each region were

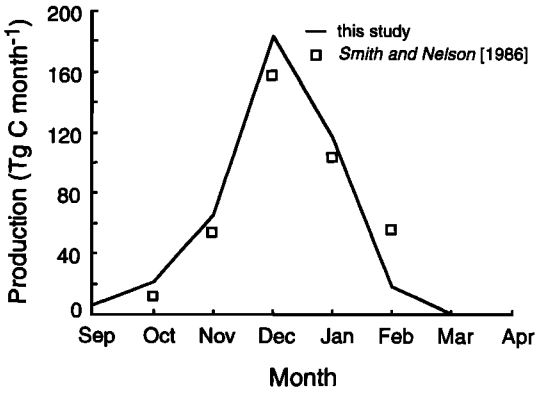

Figure 4. Comparison of monthly primary production estimates for the Antarctic MIZ made here and by *Smith and Nelson* [1986].

calculated monthly by averaging the productivity for each CZCS pixel within that region. No attempt was made to fill in CZCS data gaps. *Longhurst et al.* [1995] and *Antoine et al.* [1996] used a similar approach, defining the southern boundary of the Southern Ocean by the northern extent of sea ice each month. In contrast, *Behrenfeld and Falkowski* [1997a] defined the southern boundary of the Southern Ocean as the Antarctic coast and filled data gaps in the monthly CZCS composites (which included areas that should have remained ice covered) by interpolating spatially and temporally. *Behrenfeld and Falkowski* [1997a] also mistakenly defined the northern boundary of the Southern Ocean as 40°S rather than their stated latitude of 50°S (M. Behrenfeld, personal communication, 1997). Correcting this error decreases their estimate of Southern Ocean production from 8300 to 5471 Tg C yr^{-1}. Applying the appropriate sea ice masks to the productivity maps generated by *Behrenfeld and Falkowski* [1997a] reduces their annual production estimate by another 14% to 4787 Tg C yr^{-1}. *Behrenfeld and Falkowski* [1997a] reported that Southern Ocean production was 6900 Tg C yr^{-1} when the model of *Antoine et al.* [1996] was used in conjunction with the CZCS maps generated by *Behrenfeld and Falkowski* [1997a]. Eliminating ice-covered areas should also reduce this estimate by 14% to 5934 Tg C yr^{-1}. Although *Longhurst et al.* [1995] did not explicitly report Southern Ocean production, *Behrenfeld and Falkowski* [1997a], using data in Table 1 of *Longhurst et al.* [1995], calculated a value of 9150 Tg C yr^{-1} (rounded to 9200 in *Behrenfeld and Falkowski*'s [1997a] Table 3). This estimate included production within the South Subtropical Convergence and the New Zealand Coastal biogeochemical provinces, most of which (18.5×10^6 km^2) lie north of 50°S. All of the ice-free area below 50°S (42.5×10^6 km^2) lies within four biogeochemical provinces (Antarctic, Austral Polar, Subantarctic, and Southwest Atlantic Continental Shelf). According to *Longhurst et al.* [1995], annual production within these four biogeochemical provinces amounts to 6450 Tg C yr^{-1}. Thus the range of annual production estimates can be reduced substantially merely by applying a consistent definition for the area of the Southern Ocean (south of 50°S and north of the ice edge). A more realistic range of estimates for Southern Ocean production is probably between 4000 and 6450 Tg C yr^{-1} (Table 6).

Once the boundaries of the Southern Ocean have been consistently defined, the most important variables are, in order of their impact on estimates of primary production, Chl *a*

Table 6. Estimates of Southern Ocean Primary Production Made Using CZCS Data

Algorithm	Corrected Pigments?*	Pigment or Chl *a*†	Maximum Area, 10^6 km^2	Primary Production, Tg C yr^{-1}	Comment
Longhurst et al. [1995]	no	pigment	42.5	6450	ANTA + APLR + SANT + FKLD‡
Behrenfeld and Falkowski [1997a]	yes	pigment	41.9	4787	corrected§
Antoine et al. [1996]	no	neither	41.9	4000	
Antoine et al. [1996]	yes	pigment	41.9	5934	corrected‖
This study	yes	pigment	41.9	4414	$\rho = 1$
This study	yes	Chl *a*	41.9	3952	HPLC phaeopigments¶
This study	yes	Chl *a*	41.9	3241	fluorometric phaeopigments¶

*The CZCS underestimated pigment concentrations in the Southern Ocean by a factor of ~2 [*Sullivan et al.*, 1993]. Some algorithms corrected their CZCS imagery to reflect this underestimate using the method described by *Arrigo et al.* [1994].

†The CZCS measured pigment concentrations at the ocean surface, including nonproductive phaeopigments. "Pigment" means that the algorithm assumed that phaeopigments are negligible and that CZCS pigment was equivalent to chlorophyll *a*. "Chl *a*" means that CZCS pigment was converted to chlorophyll *a* by multiplying by an empirically derived phaeopigment:Chl *a* ratio. "Neither" means that a pigment time series for Kerguelen Island (KERFIX) was substituted for CZCS data.

‡These abbreviations refer to the biogeographical provinces defined by *Longhurst et al.* [1995], which were included in the calculation of Southern Ocean production. ANTA, Antarctic; APLR, Austral Polar; SANT, Subantarctic; FKLD, Southwest Atlantic Continental Shelf. *Behrenfeld and Falkowski* [1997a], using Table 1 of *Longhurst et al.* [1995], calculated a much higher production value for the Southern Ocean (9200 Tg C yr^{-1}). However, this estimate included the South Subtropical Convergence (SSTC) and the New Zealand Coastal (NEWZ) provinces, most of which lie north of 50°S and should not have been included in calculations of Southern Ocean production.

§The original production estimate of *Behrenfeld and Falkowski* [1997a] mistakenly extended the Southern Ocean boundary northward to 40°S, instead of 50°S as was intended. In addition, when data gaps in the monthly CZCS pigment climatologies were filled in by *Behrenfeld and Falkowski* [1997a], ice-covered areas in the Southern Ocean, where water column production should be close to zero (very little light is transmitted by sea ice), were also filled in. Production within these ice-covered regions (15×10^6 km^2 in December) was added to the monthly total. The productivity estimate was corrected here by setting the northern boundary of the Southern Ocean at 50°S and applying sea ice masks to the productivity maps generated by *Behrenfeld and Falkowski* [1997a].

‖D. Antoine recalculated the estimate of Southern Ocean production by *Antoine et al.* [1996] using the interpolated CZCS maps of *Behrenfeld and Falkowski* [1997a] as 6900 Tg C yr^{-1} [see *Behrenfeld and Falkowski*, 1997a, Table 3]. Because the ice-covered areas were filled in on these CZCS maps and because applying sea ice masks to the productivity maps of *Behrenfeld and Falkowski* [1997a] reduced the annual production estimate by 14%, the recalculated value of 6900 Tg C yr^{-1} has been reduced by a similar percentage to 5934 Tg C yr^{-1}.

¶CZCS pigments were corrected to reflect Chl *a* concentrations by multiplying by an empirically determined ratio of Chl *a* to Chl *a* plus phaeopigments. This ratio is 0.74 for fluorometrically determined phaeopigments and 0.89 for high-performance liquid chromatography (HPLC) determined phaeopigments.

concentration and maximum pigment-specific photosynthetic rate [*Behrenfeld and Falkowski*, 1997b]. Unfortunately, the pigment fields used in the various studies of primary production in the Southern Ocean vary considerably. We chose to adjust the monthly CZCS climatologies upward to reflect the fact that the measured climatological concentrations in situ are approximately a factor of 2 higher than those estimated by the global CZCS algorithm (e.g., the Southern Ocean CZCS correction [*Arrigo et al.*, 1994]). In addition, we assumed in our standard simulation that all CZCS pigment was Chl *a* contained in active phytoplankton cells (phaeopigments were negligible, $\rho = 1$ in (2)). This approach was also employed by *Behrenfeld and Falkowski* [1997a]. *Longhurst et al.* [1995], on the other hand, used the algorithm of *Sathyendranath and Platt* [1989] to estimate pigment concentrations from the CZCS, which produces pigment concentrations about a factor of 2 larger than the global CZCS algorithm [*Behrenfeld and Falkowski*, 1997b]. Fortunately, this is likely to result in pigment estimates close to those we obtained using the Southern Ocean CZCS correction. In contrast, *Antoine et al.* [1996] concluded that the monthly CZCS climatologies were unreliable in the Southern Ocean and replaced the CZCS pigments south of 50°S with a Chl *a* time series generated at the Kerguelen Island fixed station (KERFIX) near Kerguelen Island in the South Indian Ocean. *Behrenfeld and Falkowski* [1997a] showed that replacing the Kerguelen Island time series with their own "filled in" CZCS composites increased the estimate of annual production using the algorithm of *Antoine et al.* [1996] by 72.5% (from 4000 to 6900 Tg C yr^{-1} [see *Behrenfeld and Falkowski*, 1997a, Table 3]). Clearly, an input variable as important to algorithm performance as Chl *a* must be carefully defined. We believe that applying the Southern Ocean CZCS correction factor to the original CZCS climatologies and not filling in of data gaps is the most defensible approach for defining pigment distributions in the Southern Ocean using CZCS data.

There is also some disagreement regarding what fraction of the CZCS pigment signal is actually Chl *a* (i.e., what is an appropriate value for ρ in (2)). This is important because to the extent that the total pigment estimated by the CZCS consists of nonliving phaeopigments and other Chl *a* breakdown products, primary production will be proportionally overestimated. *Antoine et al.* [1996] assumed a value for ρ of 0.70, on the basis of fluorometric pigment data from 3806 hydrographic stations compiled by *Morel and Berthon* [1989]. The value for ρ was found to vary with the trophic status of the water, increasing from 0.60 for oligotrophic waters to 0.80 in eutrophic systems [*Morel and Berthon*, 1989]. It appears that ρ also may vary depending on whether phaeopigment concentration was determined fluorometrically or by high-performance liquid chromatography (HPLC). In the Ross Sea, ρ was determined to be 0.74 ($n = 582$) when pigments were determined fluorometrically, close to the mean value reported by *Morel and Berthon* [1989], but increased to 0.89 ($n = 568$) when pigments were determined by HPLC (K. R. Arrigo and M. P. Lizotte, unpublished data, 1996). Fortunately, most algorithms calculate production as a function of phytoplankton biomass and can be adjusted for the presence of phaeopigments simply by multiplying by an appropriate value for ρ. In our case, annual South-

ern Ocean production would be reduced from 4414 to 3952 Tg C yr^{-1} when applying a ρ that is determined by HPLC and to 3241 Tg C yr^{-1} when ρ is determined fluorometrically.

Other differences in the algorithm formulations and forcing fields explain only a small amount of the variation between primary productivity algorithms. For example, in those studies where productivity was assumed to be temperature dependent, one of two basic formulations has been employed: either the classic temperature versus net growth rate relationship of *Eppley* [1972], which exhibits a Q_{10} of 1.88, or the seventh-order polynomial of *Behrenfeld and Falkowski* [1997a]. The behavior of these two formulations can be compared by multiplying the *Eppley* [1972] formulation by an appropriate C:Chl *a* ratio, thus converting it to the same units as P^b_{opt} (mg C mg Chl a^{-1} hr^{-1}) used by *Behrenfeld and Falkowski* [1997a]. For the C:Chl *a* ratio of 75 used in the present study, little difference exists between these two formulations (Figure 5a), particularly at the low temperatures characteristic of the Southern Ocean (the two functions produce identical results at 2.3°C). In fact, the difference between the two formulations is <20% up to about 20°C. It should be noted, however, that the agreement between these two algorithms is highly dependent upon the C:Chl *a* ratio used. If we had used a C:Chl *a* ratio of 150 in conjunction with the temperature algorithm of *Eppley* [1972], our production estimate would have been considerably higher (Figure 5a) than the formulation used by *Behrenfeld and Falkowski* [1997a] at all temperatures.

It is unlikely that the irradiance input used to estimate production could explain the variation in the production estimates between studies, despite the different approaches used. As in the present study, *Antoine et al.* [1996] used a clear-sky radiative transfer model to estimate surface PAR as a function of time and latitude, which were subsequently adjusted to account for cloud cover. Although the cloud cover formulations differed between the two studies, they produced very similar levels of surface PAR (Figure 5b). *Behrenfeld and Falkowski* [1997a] used calculations of surface PAR provided by *Bishop et al.* [1994], which were corrected for cloud cover in a much more rigorous manner than the simple relationships employed in this study and by *Antoine et al.* [1996]. Still, estimates of surface PAR by *Bishop et al.* [1994] were very similar to estimates made using the simpler approach. Another cloud cover correction equation ($E_d = E_{dclear}\ 10^{-0.99N}$) by *Reifsnyder and Lull* [1965] also was tested but was found to attenuate surface irradiance much more strongly than the other three approaches (Figure 5b) and was not considered.

There are other differences between formulations, which are partially responsible for the range of primary production estimates generated by the various algorithms. These include the use of PAR versus PUR, the level of integration (time, depth, and wavelength), the shape of the photosynthesis versus irradiance function used, and euphotic depth calculation. The effect of many of these attributes on estimates of primary production has been discussed in depth by *Behrenfeld and Falkowski* [1997b], who concluded that they were much less important than the specification of the pigment field and maximum pigment-specific photosynthetic rate.

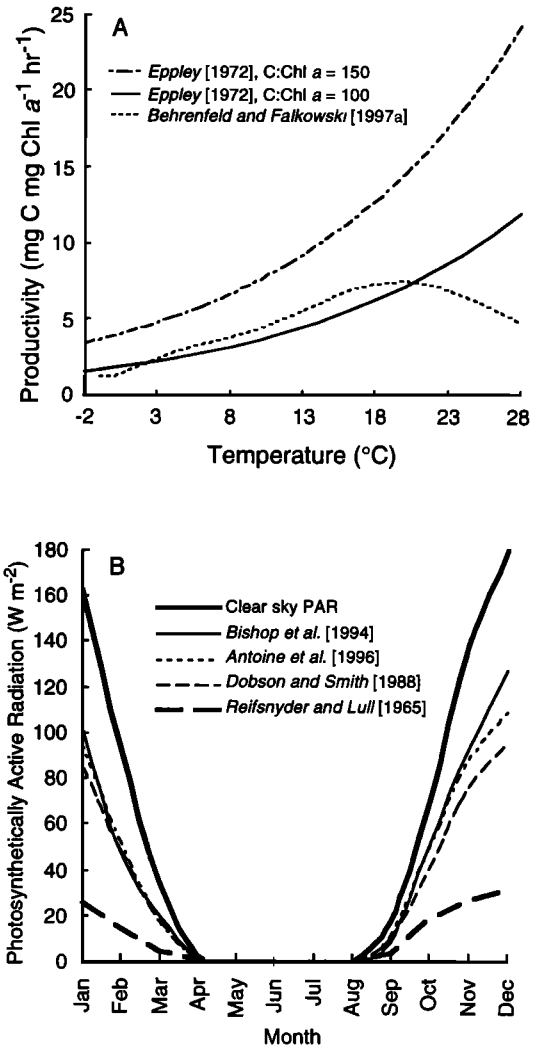

Figure 5. Comparison of (a) the temperature dependence of P^b_{opt} [*Behrenfeld and Falkowski*, 1997a] and the equivalent term in the present algorithm, G_{max} C/Chl *a* (equation (4)). If C/Chl *a* is assumed to be 50, the two algorithms produce similar results up to 20°C. (b) Comparison of a variety of techniques for obtaining cloud-corrected surface irradiance for forcing primary production algorithms at a single point in the Ross Sea (76.45°S and 172.7°E). *Bishop et al.* [1994] provide an estimate of cloud-corrected surface irradiance at 2.5° resolution, which can be used directly. An alternative approach is to apply a cloud correction algorithm to clear-sky PAR_0 (W m^{-2}) estimated using a radiative transfer model and a simple description of cloud cover, N (ranges from 0 for clear skies to 1 for complete overcast). The cloud correction algorithm used in the present study (equation (1)) and that implemented by *Antoine et al.* [1996], $PAR = PAR_0[1 - 0.29\ (N + N^2)]$, agree well with estimates of PAR by *Bishop et al.* [1994]. The algorithm of *Reifsnyder and Lull* [1965], $PAR = PAR_0\ 10^{-0.99N}$, appears to seriously underestimate surface PAR.

4.3. Spatial Variation

Spatial differences in daily rates of production presented here are consistent with previous field studies which showed that productivity is greatest near the continental shelf and declines northward. The shelf region is characterized by shallower waters and possibly the continental input of micronutrients such as iron that may limit phytoplankton growth in more remote areas [*Martin and Fitzwater*, 1988; *Martin et al.*, 1991]. Phytoplankton growth in these coastal regions is most likely controlled by upper ocean mixing rates which determine the amount of irradiance available for photosynthesis [*Mitchell and Holm-Hansen*, 1991]. *Holm-Hansen and Mitchell* [1991] ob-

served extremely high rates of primary production in the Bransfield Strait and proposed that the high productivity of the Antarctic coastal regions may help in solving the "paradox" in Antarctic waters whereby total primary production does not appear to be sufficient to sustain the complex food web. They suggested that the high rates of production, which are characteristic of the shelf areas, may more than compensate for its small size. However, our results indicate that despite its high rate of primary production, the shelf contributes <2% of the annual production of the Southern Ocean.

Rates of production in the MIZ are influenced by the degree of meltwater-induced stratification in the surface waters near retreating sea ice edges [*Smith and Nelson*, 1986]. This stratification allows the phytoplankton population to grow in a relatively high-irradiance environment. Consequently, rates of production in the MIZ are ~2–4 times greater than in the unstratified pelagic province during the spring and summer phytoplankton bloom. Previous studies estimated that primary production within the MIZ accounted for 25–30% of the total for the Southern Ocean [*Smith and Nelson*, 1986; *Legendre et al.*, 1992]. The present study suggests that the contribution by the MIZ to annual Southern Ocean production is probably closer to 10%. However, the MIZ contributes nearly 30% of annual primary production within the SIZ.

The high proportion of primary production attributed to the pelagic province is due primarily to the large size of the POOZ along with the large area of open water exposed following the annual retreat of the Antarctic sea ice. The pelagic region is characterized by deep waters and the lack of continental influence. Even though the Southern Ocean pelagic region has high concentrations of macronutrients (e.g., nitrate), it is characterized by low rates of primary production [*El-Sayed*, 1967, 1978; *Holm-Hansen et al.*, 1974]. This low productivity has been attributed to light limitation resulting from deep vertical mixing [*Mitchell and Holm-Hansen*, 1991], trace metal limitation of phytoplankton growth [*Martin and Fitzwater*, 1988; *Buma et al.*, 1991; *Martin et al.*, 1991], and grazing of phytoplankton biomass [*El-Sayed*, 1988].

4.4. Other Factors Influencing Primary Production

Sullivan et al. [1993] showed that the greatest phytoplankton abundance in the pelagic province of the Southern Ocean was located downwind and downcurrent of the major continental land masses where trace metal input would be greatest, lending credence to the hypothesis that iron limits phytoplankton growth in the open Southern Ocean. Curiously, the estimates of primary production made in the present study did not allow for trace metal limitation yet still exhibited good agreement with in situ productivity estimates in all three ecological provinces. Irradiance availability was calculated to be the primary environmental factor determining the rate of productivity in this study, suggesting perhaps that the Southern Ocean is predominantly a light-limited system. While this may be true, the present algorithm is not mechanistic enough at this time to allow a rigorous assessment of the factors that may control the growth of phytoplankton in Antarctic waters.

For example, trace metal availability was not included in the algorithm (and cannot be included at our present state of knowledge) but has been shown to be potentially important in controlling phytoplankton growth rates in other high-nutrient, low-chlorophyll (HNLC) systems [*Price et al.*, 1994]. If trace metals actually are more limiting to primary productivity in the Southern Ocean than light has been estimated to be (equation (7)), the present algorithm should have produced estimates of productivity that are higher than in situ rates. The fact that this did not happen may be explained by the fact that the C:Chl *a* ratio used in the present algorithm was at the low end of values reported for Antarctic waters [*Cota et al.*, 1992]. As can be seen in (2), when calculating productivity, a low C:Chl *a* ratio can compensate for an overestimated phytoplankton growth rate. A higher but more realistic C:Chl *a* ratio may be required if environmental factors not currently included in the productivity algorithm (e.g., iron) turn out to be more limiting to phytoplankton growth than light. Of course, this presumes that iron primarily regulates the rate of phytoplankton growth, rather than regulating phytoplankton biomass levels. If the latter is true, then the effects of iron limitation may be implicitly included in the algorithm via lower phytoplankton pigments in the CZCS data. In any case, until a more mechanistic understanding of the regulation of primary production in the Southern Ocean is achieved, the C:Chl *a* ratio of 75, which provides the best agreement between in situ and satellite-based estimates of productivity, will have to be used.

Grazing also may play an important role in regulating rates of primary production in Southern Ocean waters via its effect on phytoplankton abundance. As shown in (2), the rate of primary production is a product of phytoplankton abundance and biomass-specific growth rate. While irradiance and nutrients control the growth rate component of (2), zooplankton grazing may regulate phytoplankton biomass accumulation. It is likely that the effects of grazing are implicitly included in the CZCS imagery used to estimate phytoplankton abundance and therefore are already represented in calculations of primary production made using remotely sensed data. Consequently, it is not possible to compare estimates of production produced by the algorithm with in situ measurements to determine the importance of zooplankton grazing.

4.5. Trophic Considerations

In general, estimates of primary production for the Southern Ocean generated from CZCS data are much higher than the maximum estimate of about 1000 Tg C yr^{-1} calculated from in situ data. This is significant because 1000 Tg C yr^{-1} may be insufficient to meet even the carbon requirements of Antarctic krill, not to mention the other important grazers in the Southern Ocean such as microzooplankton, copepods, and salps. For example, estimates of krill production based upon krill biomass measurements range from 135 to 1350 Tg (wet weight) yr^{-1} [*Ross and Quetin*, 1988] or, using a wet weight:carbon ratio of 9, from 15 to 150 Tg C yr^{-1}. Assuming an ecological efficiency between phytoplankton and krill of 10% [*Pauly and Christensen*, 1995], between 150 and 1500 Tg C yr^{-1} of phytoplankton production would be required just to support the krill component of Southern Ocean heterotrophic production. Historically, it has been difficult to reconcile the large amount of upper trophic level biomass with the low rates of primary production characteristic of the Southern Ocean (the "Antarctic paradox"). However, the much higher estimates of Southern Ocean primary production estimated using CZCS data (4400–6450 Tg C yr^{-1}) are more than adequate to support upper trophic level production and suggest that there really is no Antarctic paradox with respect to trophic interactions.

A different type of trophic consideration is the amount of primary production in oceanic waters differing in trophic status (classified by phytoplankton concentration). Both *Antoine et al.* [1996] and *Behrenfeld and Falkowski* [1997a] presented sums of

annual primary production for waters classified as follows on the basis of satellite-derived pigment concentrations, C_{sat}: oligotrophic for $C_{sat} \leq 0.1$ mg m^{-3}, mesotrophic for 0.1 mg m^{-3} $> C_{sat} <$ 1.0 mg m^{-3}, or eutrophic for $C_{sat} \geq 1.0$ mg m^{-3}. They estimated that of annual global primary production, 24–39% occurs in oligotrophic areas, 55–61% occurs in mesotrophic areas, and 6–15% occurs in eutrophic areas. *Behrenfeld and Falkowski* [1997a] noted that excluding the polar and subpolar regions (latitudes >50°S) shifted the oligotrophic value up and the eutrophic value down by 5% each. We can elaborate on this shift for the Southern Ocean by noting that <0.1% of the Southern Ocean would be classified as oligotrophic, and thus the primary production in oligotrophic waters was insignificant. The Southern Ocean primary production occurs mostly in mesotrophic waters (68% of the total), but eutrophic waters (32%) contribute more than twice the portion estimated for the global ocean. Thus, where and when the Southern Ocean is ice free, it is generally of higher trophic status than the world ocean.

Notation

λ	wavelength, nm.
$E_d(\lambda)$	downwelling irradiance, W m^{-2} nm^{-1}, μmol photons m^{-2} s^{-1} nm^{-1}.
$E_{dclear}(\lambda)$	clear-sky downwelling irradiance, W m^{-2} nm^{-1}, μmol photons m^{-2} s^{-1} nm^{-1}.
R	surface reflection, dimensionless.
$a_w(\lambda)$	absorption coefficient for pure seawater, m^{-1}.
$a_d(\lambda)$	absorption coefficient for detritus, m^{-1}.
$a_c^*(\lambda)$	Chl a-specific absorption coefficient for phytoplankton, m^2 mg^{-1} Chl a.
$b_{bw}(\lambda)$	backscattering coefficient for pure seawater, m^{-1}.
$b_{bp}(\lambda)$	backscattering coefficient for particulates, m^{-1}.
μ	mean cosine of underwater irradiance distribution, dimensionless.
N	fractional cloud cover, dimensionless.
PP_{EU}	primary production within the euphotic zone, mg C m^{-2} d^{-1}.
C	carbon, mg m^{-3}.
Chl a	chlorophyll a concentration, mg m^{-3}.
ρ	Chl a/(Chl a + phaeopigments), dimensionless.
G	net biomass-specific growth rate, hour^{-1}.
G_0	net biomass-specific growth rate at 0°C, 0.59 hour^{-1}.
G_{max}	maximum temperature-dependent net biomass-specific growth rate, hour^{-1}.
z	depth, m.
t	time, hour.
T	temperature, °C.
r	constant = 0.0633, °C^{-1}.
r_{lim}	resource limitation term, dimensionless.
N_{lim}	nutrient limitation term, dimensionless.
L	light limitation term, dimensionless.
PUR	photosynthetically usable radiation, μmol photons m^{-2} s^{-1}.
PUR*	average daily photosynthetically usable radiation, μmol photons m^{-2} s^{-1}.
E_k'	spectral photoadaptation parameter, μmol photons m^{-2} s^{-1}.
$E_{k\,max}'$	maximum value for E_k', 80 μmol photons m^{-2} s^{-1}.
a_{cmax}^*	maximum value for $a_c^*(\lambda)$, m^2 mg^{-1} Chl a.

Acknowledgments. This work was supported by NASA grants 971-438-20-10 and 971-148-65-56 to Kevin Arrigo and NSF grant OPP 95-25805 to Kevin Arrigo and Mike Lizotte. We are grateful to Steve Fiegles for providing us with the most recent version of the SMMR data for creating our sea ice masks and to Mike Martino for providing the Antarctic land mask. We would also like to thank Dale Robinson for his comments on earlier versions of the manuscript.

References

Antoine, D., J.-M. Andre, and A. Morel, Oceanic primary production, 2, Estimation at global scale from satellite (coastal zone color scanner) chlorophyll, *Global Biogeochem. Cycles*, *10*, 57–69, 1996.

Arrigo, K. R., and C. W. Sullivan, A high resolution bio-optical model of microalgal growth: Tests using sea ice algal community time series data, *Limnol. Oceanogr.*, *39*, 609–631, 1994.

Arrigo, K. R., C. R. McClain, J. K. Firestone, C. W. Sullivan, and J. C. Comiso, A comparison of CZCS and in situ pigment concentrations in the Southern Ocean, *NASA Tech. Memo.*, *104566*, 30–34, 1994.

Arrigo, K. R., D. L. Worthen, P. Dixon, and M. P. Lizotte, Primary productivity of near surface communities within Antarctic pack ice, in *Antarctic Sea Ice: Biological Processes, Interactions and Variability*, *Antarct. Res. Ser.*, vol. 73, edited by M. P. Lizotte and K. R. Arrigo, pp. 23–43, AGU, Washington, D. C., 1998.

Behrenfeld, M. J., and P. G. Falkowski, Photosynthetic rates derived from satellite-based chlorophyll concentration, *Limnol. Oceanogr.*, *42*, 1–20, 1997a.

Behrenfeld, M. J., and P. G. Falkowski, A consumer's guide to phytoplankton primary productivity models, *Limnol. Oceanogr.*, *42*, 1479–1491, 1997b.

Bishop, J. K. B., J. McLaren, G. Zulema, and W. B. Rossow, Documentation and description of solar irradiance data sets for SeaWiFS: NASA grant NAGW no. 2189, internal document, Goddard Inst. for Space Stud., New York, 1994.

Brightman, R. I., and W. O. Smith Jr., Photosynthesis-irradiance relationships of Antarctic phytoplankton during austral winter, *Mar. Ecol. Prog. Ser.*, *53*, 143–151, 1989.

Buma, A. G. J., H. J. W. De Baar, R. F. Nolting, and A. J. Van Bennekom, Metal enrichment experiments in the Weddell-Scotia seas: Effects of iron and manganese on various plankton communities, *Limnol. Oceanogr.*, *36*, 1865–1878, 1991.

Bunt, J. S., Microalgae of the Antarctic pack ice zone, in *Symposium on Antarctic Oceanography*, edited by R. I. Curie, pp. 198–218, Scott Polar Res. Inst., Cambridge, England, 1968.

Bunt, J. S., Microbial productivity in polar regions, in *Microbes and Biological Productivity*, edited by D. E. Hughes and A. H. Rose, *Symp. Soc. Gen. Microbiol.*, *21st*, 332–354, 1971.

Comiso, J. C., C. R. McClain, C. W. Sullivan, J. P. Ryan, and C. L. Leonard, Coastal zone color scanner pigment concentrations in the Southern Ocean and relationships to geophysical surface features, *J. Geophys. Res.*, *98*, 2419–2451, 1993.

Cota, G. F., W. O. Smith, and N. M. Nelson, Nutrient and biogenic particulate distributions, primary productivity and nitrogen uptake in the Weddell-Scotia Sea marginal ice zone during winter, *J. Mar. Res.*, *50*, 155–181, 1992.

da Silva, A., C. C. Young, and S. Levitus, *Atlas of Surface Marine Data 1994*, vol. 1, *Algorithms and Procedures*, *NOAA Atlas NESDIS 6*, 83 pp., Natl. Oceanogr. Data Cent., Silver Spring, Md., 1994.

Dobson, F. W., and S. D. Smith, Bulk models of solar radiation at sea, *Q. J. R. Meteorol. Soc.*, *114*, 165–182, 1988.

El-Sayed, S. Z., Prospects of primary productivity studies in Antarctic waters, paper presented at the SCAR Symposium on Antarctic Oceanography, Sci. Comm. on Antarct. Res., Santiago, Chile, September 13–16, 1966.

El-Sayed, S. Z., On the productivity of the southwest Atlantic Ocean and the waters west of the Antarctic Peninsula, in *Biology of the Antarctic Seas III*, *Antarct. Res. Ser.*, vol. II, edited by G. A. Llano and W. L. Schmitt, pp. 15–47, AGU, Washington, D. C., 1967.

El-Sayed, S. Z., Primary productivity and estimates of potential yields of the Southern Ocean, in *Polar Research*, edited by M. A. McWhinnie, pp. 141–160, Westview, Boulder, Colo., 1978.

El-Sayed, S. Z., Seasonal and interannual variabilities in Antarctic phytoplankton with reference to krill distribution, in *Antarctic Ocean and Resources Variability*, edited by D. Sahrhage, pp. 101–119, Springer-Verlag, New York, 1988.

El-Sayed, S. Z., and E. F. Mandelli, Primary production and standing

crop of phytoplankton in the Weddell Sea and Drake Passage, in *Biology of the Antarctic Seas, II, Antarct. Res. Ser.*, vol. 5, edited by G. A. Llano, pp. 87–106, AGU, Washington, D. C., 1965.

Eppley, R. W., Temperature and phytoplankton growth in the sea, *Fish. Bull., 70*, 1063–1084, 1972.

Gloersen, P., W. J. Campbell, D. J. Cavalieri, J. C. Comiso, C. L. Parkinson, and H. J. Zwally, *Arctic and Antarctic Sea Ice, 1978–1987*, 290 pp., Natl. Aeronaut. and Space Admin., Washington, D. C., 1992.

Gregg, W. W., and K. L. Carder, A simple spectral solar irradiance model for cloudless maritime atmospheres, *Limnol. Oceanogr., 35*, 1657–1675, 1990.

Holm-Hansen, O., and B. G. Mitchell, Spatial and temporal distribution of phytoplankton and primary production in the western Bransfield Strait region, *Deep Sea Res., Part A, 38*, 961–980, 1991.

Holm-Hansen, O., S. El-Sayed, G. A. Franchesini, and R. L. Cuhel, Primary production and factors controlling phytoplankton growth in the Southern Ocean, paper presented at the Third SCAR Symposium on Antarctic Biology, Sci. Comm. on Antarct. Res., Washington, D. C., Aug. 26–30, 1974.

Jennings, J. C., L. I. Gordon, and D. M. Nelson, Nutrient depletion indicates high primary productivity in the Weddell Sea, *Nature, 309*, 51–54, 1984.

Legendre, L., S. F. Ackley, G. S. Dieckmann, B. Gullicksen, R. Horner, T. Hoshiai, I. A. Melnikov, W. S. Reeburgh, M. Spindler, and C. W. Sullivan, Ecology of sea ice, 2, Global significance, *Polar Biol., 12*, 429–444, 1992.

Levitus, S., R. Burgett, and T. P. Boyer, *World Ocean Atlas 1994*, vol. 3, *Salinity, NOAA Atlas NESDIS 3*, 111 pp., Natl. Oceanogr. Data Cent., Silver Spring, Md., 1994.

Lizotte, M. P., and K. R. Arrigo, Parameterization of a spectral model of primary production in the Southern Ocean (abstract), *Eos Trans. AGU, 75*(3), Ocean Sci. Meet. Suppl., 217, 1994.

Longhurst, A., S. Sathyendranath, T. Platt, and C. Caverhill, An estimate of global primary production in the ocean from satellite radiometer data, *J. Plankton Res., 17*, 1245–1271, 1995.

Martin, J. H., and S. E. Fitzwater, Iron deficiency limits phytoplankton growth in the northeast Pacific Subarctic, *Nature, 331*, 341–343, 1988.

Martin, J. H., M. Gordon, and S. E. Fitzwater, The case for iron, *Limnol. Oceanogr., 36*, 1793–1802, 1991.

McClain, C. R., K. R. Arrigo, K.-S. Tai, and D. Turk, Observations and simulations of physical and biological processes at ocean weather station P, 1951–1980, *J. Geophys. Res., 101*, 3697–3713, 1996.

Mitchell, B. G., and O. Holm-Hansen, Bio-optical properties of Antarctic Peninsula waters: differentiation from temperate ocean models, *Deep Sea Res., Part A, 38*, 1009–1028, 1991.

Monod, J., *Recherches sur la croissance des cultures bacteriennes*, Herman et Cie, Paris, 1942.

Morel, A., Available, usable, and stored radiant energy in relation to marine photosynthesis, *Deep Sea Res., 25*, 673–688, 1978.

Morel, A., and J.-F. Berthon, Surface pigments, algal biomass profiles and potential production of the euphotic layer: Relationships reinvestigated in view of remote sensing applications, *Limnol. Oceanogr., 34*, 1545–1562, 1989.

Pauly, D., and V. Christensen, Primary production required to sustain global fisheries, *Nature, 374*, 255–257, 1995.

Price, N. M., B. A. Ahner, and F. M. M. Morel, The equatorial Pacific: Grazer controlled phytoplankton populations in an iron-limited ecosystem, *Limnol. Oceanogr., 39*, 520–534, 1994.

Reifsnyder, W. E., and H. W. Lull, Radiant energy in relation to forests, *Tech. Bull. U.S. Dep. Agric., 1344*, 17 pp., 1965.

Ross, R. M., and L. B. Quetin, *Euphausia superba*: A critical review of annual production, *Comp. Biochem. Physiol. B, Comp. Biochem., 90B*, 499–505, 1988.

Ryther, J. H., Geographic variations in productivity, in *The Composition of Sea Water and Comparative and Descriptive Oceanography, The Sea*, vol. 2, edited by M. N. Hill, pp. 347–380, John Wiley, New York, 1963.

Sakshaug, E., and O. Holm-Hansen, Factors governing pelagic production in polar oceans, in *Marine Phytoplankton and Productivity*, edited by O. Holm-Hansen, L. Bolis, and R. Gilles, pp. 1–18, Springer-Verlag, New York, 1984.

Sathyendranath, S., and T. Platt, Remote sensing of ocean chlorophyll: consequences of non-uniform pigment profile, *Appl. Opt., 28*, 490–495, 1989.

Smith, W. O., and D. M. Nelson, The importance of ice-edge phytoplankton production in the Southern Ocean, *BioScience, 36*, 251–257, 1986.

Smith, W. O., N. K. Keene, and J. C. Comiso, Interannual variability in estimated primary productivity of the Antarctic marginal ice zone, in *Antarctic Ocean and Resources Variability*, edited by D. Sahrhage, pp. 131–139, Springer-Verlag, New York, 1988.

Sullivan, C. W., K. R. Arrigo, C. R. McClain, J. C. Comiso, and J. Firestone, Distributions of phytoplankton blooms in the Southern Ocean, *Science, 262*, 1832–1837, 1993.

Tilzer, M. M., M. Elbrachter, W. W. Gieskes, and B. Beese, Light-temperature interactions in the control of photosynthesis in Antarctic phytoplankton, *Polar Biol., 5*, 105–111, 1986.

Wilson, D. L., W. O. Smith Jr., and D. M. Nelson, Phytoplankton bloom dynamics of the western Ross Sea ice-edge, I, Primary productivity and species-specific production, *Deep Sea Res., Part A, 33*, 1375–1387, 1986.

K. R. Arrigo, Oceans and Ice Branch, NASA Goddard Space Flight Center, Code 971.0, Greenbelt, MD 20771. (e-mail: kevin@shark.gsfc.nasa.gov)

M. P. Lizotte and A. Schnell, Department of Biology and Microbiology, University of Wisconsin Oshkosh, Oshkosh, WI 54901-8640.

D. Worthen, Science Systems and Applications, Inc., Lanham, MD 20706.

(Received October 23, 1997; revised March 2, 1998;
accepted March 19, 1998.)